RSC Advances

PAPER

View Article Online
View Journal | View Issue

Cite this: *RSC Adv.*, 2018, **8**, 11163

Identification of a new series of benzothiazinone derivatives with excellent antitubercular activity and improved pharmacokinetic profiles†

Lu Xiong,‡[a] Chao Gao,‡*[a] Yao-Jie Shi,[a] Xin Tao,[a] Juan Rong,[a] Kun-Lin Liu,[a] Cui-Ting Peng,[ab] Ning-Yu Wang,[c] Qian Lei,[a] Yi-Wen Zhang,[a] Luo-Ting Yu *[a] and Yu-Quan Wei[a]

Received 24th January 2018
Accepted 8th March 2018

DOI: 10.1039/c8ra00720a

rsc.li/rsc-advances

Nitrobenzothiazinone (BTZ) is a promising scaffold with potent activity against *M. tuberculosis* by inhibiting decaprenylphosphoryl-beta-D-ribose 2′-oxidase (DprE1). But unfavorable durability poses a challenge to further development of this class of agents. Herein, a series of BTZs bearing a variety of different substituents at the C-2 position were designed and synthesized. Compounds were screened for their antimycobacterial activity against *Mycobacterium tuberculosis* H37Ra and were profiled for metabolic stability, plasma protein-binding capacity and pharmacokinetics *in vivo*. In general, these new BTZs containing *N*-piperazine, *N*-piperidine or *N*-piperidone moiety have excellent antitubercular activity and low cytotoxicity. Several of the compounds showed improved microsomal stability and lower plasma protein-binding, opening a new direction for further lead optimization. And we obtained compound **3o**, which maintained good anti-tuberculosis activity (MIC = 8 nM) and presented better *in vitro* ADME/T and *in vivo* pharmacokinetic profiles than reported BTZ compound **PBTZ169**, which may serve as a candidate for the treatment of tuberculosis.

1 Introduction

Tuberculosis (TB) is one of the top ten causes of death worldwide, a major disease causing 1.3 million deaths every year and represents the leading cause of mortality resulting from a bacterial infection.[1] Furthermore, with the sprawl of multi-drug resistant–TB (MDR–TB) and rifampicin resistant–TB (RR–TB), it causes nearly 50% mortality in treated individuals, and this disease threatens people's health seriously (http://www.who.int/tb/publications/global_report/archive/en/). The currently recommended treatment for cases of drug-susceptible TB is a 6-month regimen of four first-line drugs: isoniazid (INH), rifampicin (RIF), ethambutol (EMB) and pyrazinamide (PZA), which is followed by a longer phase of treatment with RIF and INH to eradicate the remaining bacilli which entered into a dormant, slowly replicating latent phase.[2] While, the latest data reported by WHO showed the treatment success rate for MDR–TB is 54%, reflecting high rates of treatment failure.[3]

Nitrobenzothiazinone (BTZ), represented by **BTZ043** (Fig. 1a) and **PBTZ169** (Fig. 1b), is one of the most promising scaffolds in the antitubercular drug pipelines with nanomolar concentrations against both sensitive-TB and MDR–TB.[4–6] The nitro group at position 8 of BTZ is critical for antituberculosis activity.[7] BTZs undergo nitroreduction to form a nitroso derivative, which then covalently reacts with cysteine 387 (C387) residue of decaprenylphosphoryl-β-*d*-ribose (DPR) 2′-oxidase (DprE1). DprE1 enzyme catalyzes biosynthesis of a prenylphosphoryl-β-D-arabinose (DPA), which is an essential process for the mycobacteria cell wall assembly.[8–10] **BTZ043** and **PBTZ169** are undergoing extensive preclinical studies and phase II clinical trials, respectively.[2,11]

Pharmacokinetic profile showed positive correlation with *in vivo* efficacy.[12] Effort to improve pharmacokinetic properties in

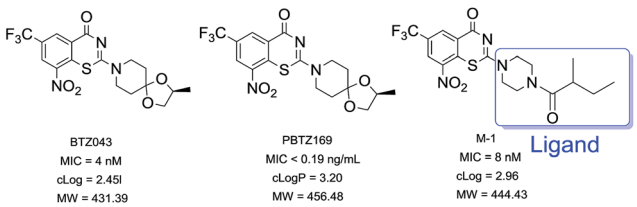

Fig. 1 (a) BTZ043 (b) PBTZ169 (c) hit compound M-1.

[a]*State Key Laboratory of Biotherapy and Cancer Center, West China Hospital, Sichuan University and Collaborative Innovation Center, Chengdu 610041, China. E-mail: yuluot@scu.edu.cn; gaochao527@hotmail.com; Fax: +86 28 8516 4060; Tel: +86 28 8516 4063; +86 13550095023*

[b]*Department of Pharmaceutical and Bioengineering, School of Chemical Engineering, Sichuan University, Chengdu, Sichuan 610065, China*

[c]*School of Life Science and Engineering, Southwest JiaoTong University, Sichuan 611756, China*

† Electronic supplementary information (ESI) available. See DOI: 10.1039/c8ra00720a

‡ These authors contributed equally.

the early drug discovery process is essential to minimize the attrition rate during the pre-clinical and clinical development phases. It has been discovered that **BTZ043** and **PBTZ169** displayed similar pharmacokinetic properties,[5] and exhibited unfavorable metabolic stability in our tests (Table 4). It poses a challenge to drug formulation as well as other aspects of clinical studies during the continuing development of this promising class of antitubercular agents. Some work to improve the pharmacokinetic properties of **BTZ043** and **PBTZ169** has been reported.[13–15] And in our previous study, we synthesized a series of 4-carbonyl piperazine substituted 1,3-benzothiazin-4-one derivatives and most of these compounds exhibited good antitubercular activities and favorable aqueous solubility. However, the bioavailability of hit compound **M-1** (Fig. 1c) (*F* 8.6%) was not improved compared with **BTZ043** (*F* 29.5%), which may result from hydrolysis of the amide group. Therefore, we synthesized new series of BTZs with alternative groups at position 2. Our focus was to improve the metabolic stability of this kind of scaffold and maintain good *in vitro* potency by medicinal chemistry strategy simultaneously. Here, we present results of the SAR analyses along with our efforts toward elucidation of the improvement of pharmacokinetic profiles.

2 Results and discussion

2.1 Synthesis

2.1.1 An overview of nitrobenzothiazinone synthesis. The structural variation on hit compound **M-1** was divided into coupling with four series linkers. The synthesis of core nitrobenzothiazinone was achieved by utilizing efficient one-pot three-step reaction as outline in Scheme 1. A reaction of 2-chloro-3-nitro-5-(trifluoromethyl) benzoic acid in dichloromethane with oxalyl chloride and catalyst DMF gave 2-chloro-3-nitro-5-(trifluoromethyl)benzoyl chloride. The intermediate was prepared from 2-chloro-3-nitro-5-(trifluoromethyl)benzoyl chloride and ammonium thiocyanate in dichloromethane using 18-Crown-6 as a phase-transfer catalyst (PCT). Next, the appropriate heterocyclic amines nucleophilic attacked on the isothiocyanato group. Due to the presence of two electron-withdrawing groups in the *para* and *ortho* position of the chlorine atom, respectively, it was then cyclization to the desired benzothiazine-4-ones from the sulfur heterocyclization (Scheme 1).

2.1.2 Synthesis of amine derivatives. Detailed synthetic pathways to amine derivatives **21–22**, **41–48** and **49–58** which are commercially unavailable are depicted in Scheme 2. For rapid SAR exploration, a parallel synthesis route was designed that would enable preparation of various analogues with minimum purification. Coupling of **1–4** with Boc-glycine yielded **9–12** in the presence of *N*-(3-dimethylaminopropyl)-*N*′-ethylcarbodimide hydrochloride diethyl azodicarboxylate (EDCI) and 1-hydroxybenzotriazole (HOBT) followed by treatment with trifluoroacetic acid in dichloromethane. 4-Nitrobenzenesulfonyl chloride was dropped into a suspension of the trifluoroacetate and trimethylamine at 0 °C bath in dichloromethane to give the desired acetamide **13–16**, then the piperazinones (**17–20**) were formed by further reaction with 1,2-dibromoethane. Treatment of **17–20** with methyl-mercaptopropionate in acetonitrile/DMSO (v/v 49/1) at 50 °C gave the desired compounds (**21–24**) in 69.06% overall yield starting from **1–4**. Analogue **41–48** was synthesized from the corresponding benzoyl chloride (**25–32**) in 73.02% yield over two steps as shown in Scheme 2 *via* nucleophilic substitution of compounds **25–32** with 1-Boc-4-hydroxypiperidine followed by deprotection the Boc-group. Reaction mixture evaporated, dissolved in methyl alcohol. Triethylamine was added to the solution followed by removal of the solvent *in vacuo* to give yellow solid, which was used to synthesis of **2h–2o.**

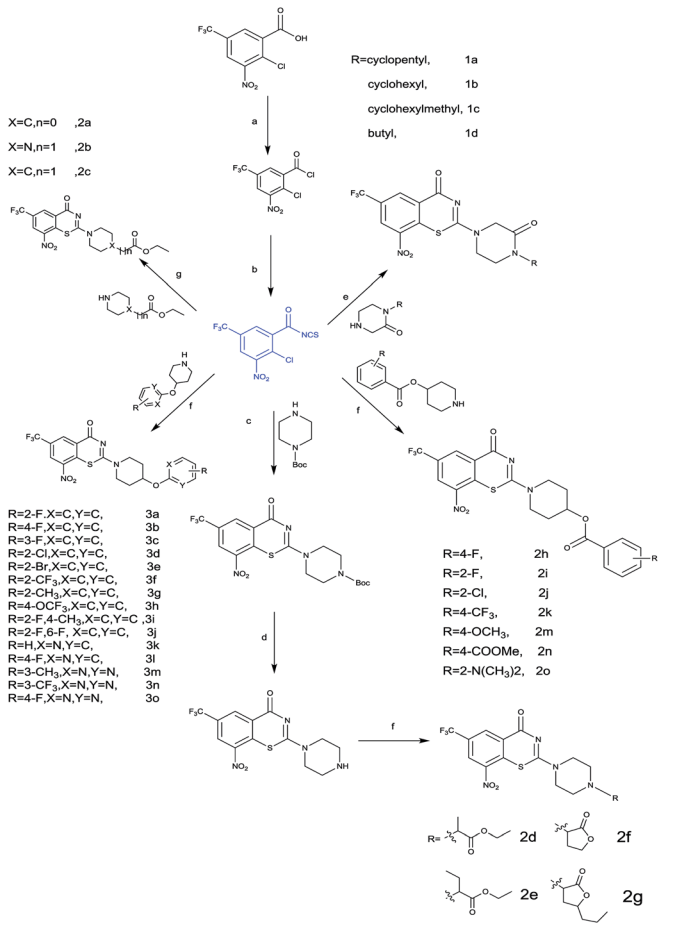

Scheme 1 Synthesis of nitrobenzothiazinone derivative: (a) cat. DMF, oxalyl chloride, DCM, rt; (b) cat. 18-crown-6, NH_4SCN, DCM, rt; (c) *tert*-butyl piperazine-1-carboxylate, DCM, rt; (d) cat. TFA, DCM, rt; (h) cat. K_2CO_3, ester, dry DMF, 60 °C, 3 h; (e) 1a5-1d5, DCM, rt; (f) DCM, rt. (g) cat. K_2CO_3, ester, dry DMF, 60 °C 3 h.

Coupling of 1-Boc-4-hydroxypiperidine with phenol (**49–58**) in the presence of diethyl azodicarboxylate (DEAD) and PPh3 followed by treatment with trifluoroacetic acid (TFA) in dichloromethane gave **69–78** in 5–70% yield.

Intermediates **83**, **84** were obtained from 2-bromopyridine in two steps. First, condensation of 1-Boc-4-hydroxypiperidine with sodium hydride in dry DMF, and then treatment of 2-bromopyridine (**79**, **80**) furnished **81** and **82.** The Boc-group was deprotected by TFA (trifluoroacetic acid) to afford **83** and **84.** Similarly, this condition was also used to produce **91–93** with

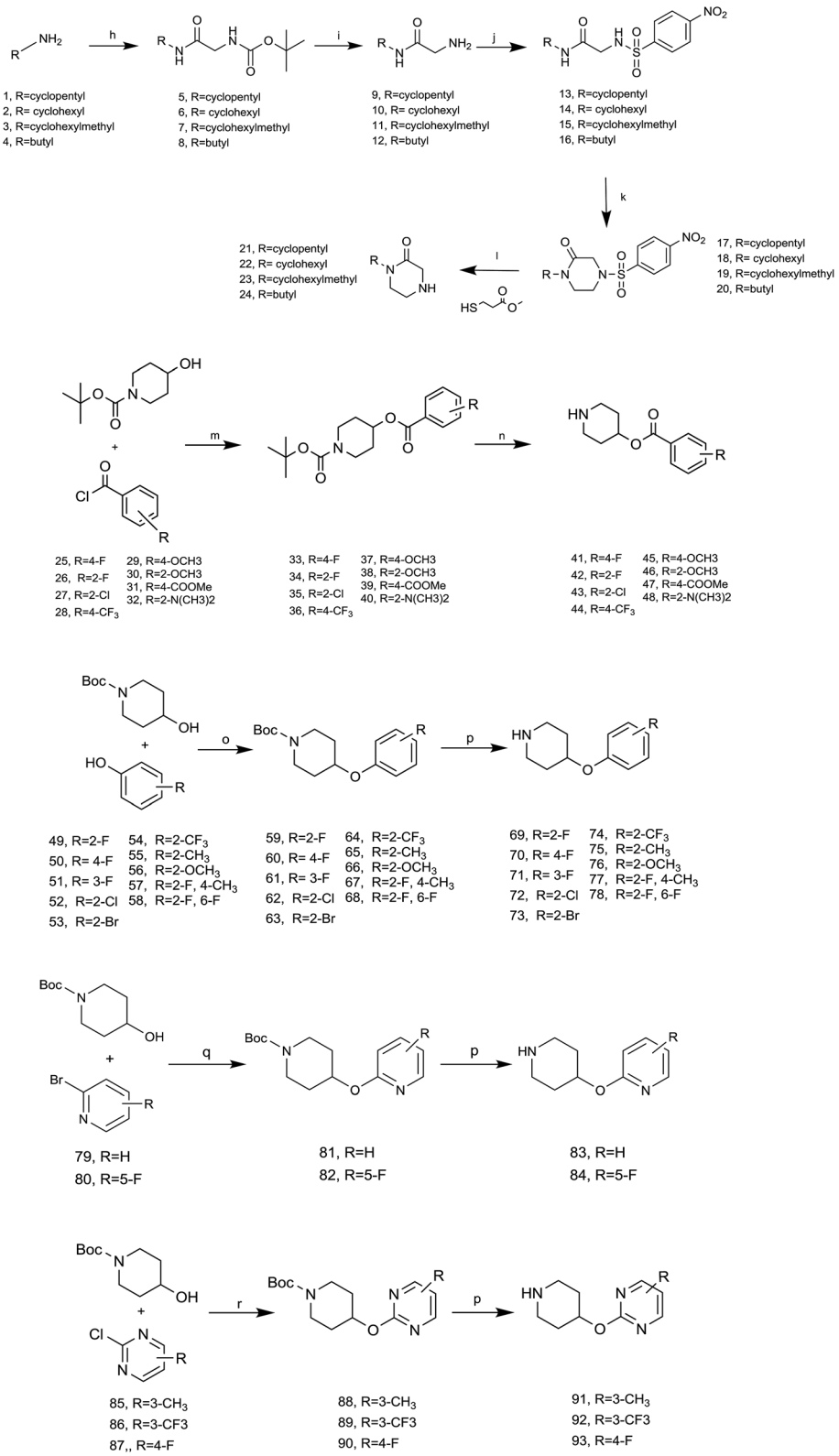

Scheme 2 Synthesis of amine derivatives: (h) cat. EDCI, HOBT, Boc-glycine, DCM, rt.12 h; (i) cat. TFA, DCM, rt, 1 h; (j) cat. TEA, 4-nitro-benzenesulfonyl chloride, 0 °C, 0.5 h, rt, 6 h; (k) cat. K_2CO_3, 1,2-dibromoethane, DMF, 60 °C; (l) cat. LiOH, methyl-mercaptopropionat, CAN/DMSO (v/v = 49/1), 50 °C, 6 h; (m) cat. TEA, DCM, rt; (n) cat. TFA, DCM, 0 °C, 0.5 h, rt, 1.5–4 h; reagents and conditions: (o) cat. PPh3, DEAD, THF, rt; (p) cat. TFA, DCM, rt; (q) cat. NaH, dry DMSO, rt, 0 °C, 0.5 h, rt; (r) cat. NaH, dry DMF, 0 °C, 0.5 h, rt.

Table 1 SAR of analogues[a]

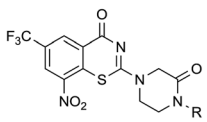

1a-1d

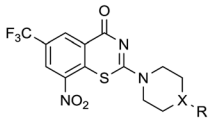

2a-2o

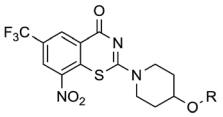

3a-3o

Compd	X	R	MIC (nM)	clog *P*	Aqueous solubility (μg mL^{-1})	CC50 (Vero) μMb	Compd	X	R	MIC (nM)	clog *P*	Aqueous solubility (μg mL^{-1})	CC50 (Vero) μMb
1a	—		13	3.52	7.37	>10	**2n**	C	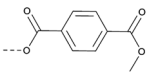	63	4.15	ND	>10
1b	—		17	4.08	1.63	>10	**2o**	C	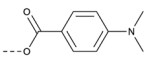	31	4.66	ND	>10
1c	—		17	4.79	3.57	>10	**3a**	—		16	4.21	0.5	>10
1d	—		34	49.56	3.57	>10	**3b**	—	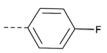	≤2	4.42	<1	>10
2a	C	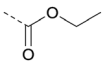	8	2.78	ND	>10	**3c**	—		31	4.42	ND	>10
2b	N	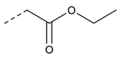	20	3.23	ND	>10	**3d**	—		31	4.76	ND	>10
2c	C	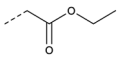	16	3.40	ND	>10	**3e**	—		31	4.91	ND	>10
2d	N	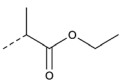	8	3.54	ND	>10	**3f**	—		4	5.26	ND	>10
2e	N	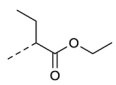	31	4.07	ND	>10	**3g**	—		16	4.63	ND	>10
2f	N	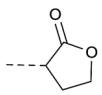	64	1.76	ND	>10	**3h**	—	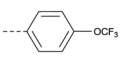	8	5.33	ND	>10
2g	N	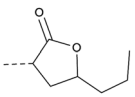	16	3.40	ND	>10	**3i**	—	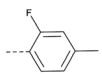	16	4.71	1	>10
2h	C	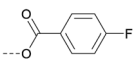	≤2	4.33	ND	>10	**3j**	—		125	4.21	ND	>10
2i	C	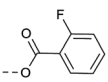	4	3.89	ND	>10	**3k**	—		31	3.54	ND	>10
2j	C	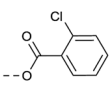	8	4.46	ND	>10	**3l**	—	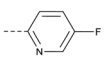	31	3.72	ND	>10
2k	C	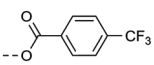	8	5.07	ND	>10	**3m**	—		31	3.21	2.39	>10
2l	C	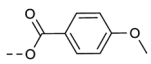	8	4.36	ND	>10	**3n**	—		4	3.63	1.73	>10

Table 1 (*Contd.*)

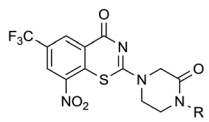
1a-1d

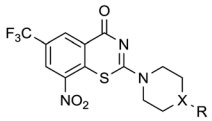
2a-2o

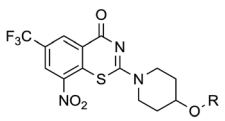
3a-3o

Compd	X	R	MIC (nM)	clog *P*	Aqueous solubility (μg mL^{-1})	CC50 (Vero) μMb
2m	C	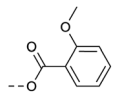	63	4.12	ND	>10
BTZ043			4	2.45	<1	>10

Compd	X	R	MIC (nM)	clog *P*	Aqueous solubility (μg mL^{-1})	CC50 (Vero) μMb
3o	—		8	2.87	5.14	>10

[a] ND: not determined. [a]clog *P* was calculate by Chembiodraw Ultra version 11.0. [b]Cytotoxicityagainst kidney epithelial cells extracted from an African green monkey (VERO). Dash indicates that the value was not relevant.

acyl chloride (**85–87**). All target compounds and intermediates were characterized by ^{1H}NMR and LC-MS.

2.2 Biological evaluation

2.2.1 *In vitro* antimycobacterial activity. Compounds prepared in this manner were tested the against M.*tb* H37Ra medium using the standard broth micro dilution method and minimum inhibitory concentration (MIC) values determined at 7 days.[16] Kinetic solubility of the test compounds was determined in different pH conditions/mediums, and apparent permeability (P_{app}) of test compounds was determined by using MDKI-MDCKII cells.[17] Metabolic stabilities of selected compounds in human, rat, and mouse liver microsomes were assessed by incubating for 30 min and measuring the percentage of compound remaining. CYP inhibition potential was determined using the following recombinant microsomes:[18] CYP1A2, CYP2C9, CYP2C19, CYP2D6 and CYP3A4. SD rats were used to determine Pharmacokinetic parameters and the experimental data was analyzed by WinNonlin V6.2.1.

Initial medicinal chemistry strategy was to replace amido bond with C–N bond for improving the metabolic stability. First the piperazinone derivatives were synthesized as lactam is the main metabolite of cyclic amine. The introduction of oxygen atom also served as a hydrogen-bond acceptor[19] (Table 1). Cyclopentyl piperazinone **1a** showed best anti-M.*tb* activity (MIC = 13 nM). To further explore the effect of the ring size, we synthesized a 6-membered aliphatic cyclic which led to a slightly loss of activity. No anti-M.*tb* activity difference was observed in homologs cyclohexyl (**2b**) and cyclohexylmethyl (**2c**) substitution. A replacement of cycloalkyl-substitution with linear butyl group **2d** caused a drastic increase on aqueous solubility (49.56 μg mL^{-1}) resulted from molecular flexibility enhancement.[20] However, further investigation of butyl substitute **2d** was suspended because of the potential metabolic instability of alkyl group *in vivo*.[21]

Then piperazine and piperidine derivatives were also designed and synthesized (Table 2). The alkyl esters exhibited good anti-M.*tb* activity and acceptable solubility. The compound **2a** ethyl formate showed good anti-M.*tb* activity (8 nM). The analogues of **2a** with four-carbon atoms ester linker (**2b**) showed a reduced activity (MIC = 20 nM). Interestingly, this effect could be balanced with an introduction of methyl on α-C of the carbonyl group (**2d**, MIC = 8 nM). Compound **2d** maintained anti-M.*tb* activity with dramatic improvement on solubility (27.07 μg mL^{-1} in pH 6.5, 84.16 μg mL^{-1} in pH 2.0) compared with **BTZ043**, probably due to the disruption of molecule planarity.[22] A significant reduced activity could be observed when the 2-methyl was changed to 2-ethyl (**2e**, MIC = 31 nM) or lactone (**2f**, MIC = 64 nM). And introduction of alkyl on the lactone ring led to obvious enhanced potency (**2g** *vs.* **2f**). Compound **2c** showed the same range of activity (MIC = 16 nM) as compound **2b** (MIC = 20 nM), suggesting similar effect of piperidine and piperazine on activity. Next, we turned our attention to the aryl esters. Aryl analogues with small halogens (**2h**, **2i**, and **2j**) were all maintained good anti-M.*tb* activity, in particular compound **2i** with a low value of MIC ≤2 nM. *para*-Methoxy-substitution (**2l**) was favored over *ortho* (**2m**) substituted analogues. While, bulk groups such as ester group (**2n**, MIC = 63 nM) and dimethylamino (**2o**, MIC = 31 nM) resulted in a significant drop in activity.

In consideration of metabolic instability of ester group,[23] compounds with 4-oxypiperidyl moiety **3a–3o** were designed and synthesized (Table 3). Similarly, we initially explored the effect of adding small halogens to the benzene ring. Benzyl analogue with fluoro-substitution (**3a**) was favored over chlorine-substitution (**3d**) and bromine-substitution (**3e**) analogues. Furthermore, *meta* substitution (**3c**) showed the best anti-M.*tb* activity (MIC ≤ 2 nM) relative to *ortho* (**3a**, MIC = 16 nM) and *para* (**3b**, MIC = 4 nM) substitution. The methyl, trifluoromethyl and trifluoromethoxy derivatives (**3g**, **3f** and **3h**) showed good activities and disubstituted groups (**3i**, **3g**) were

Table 2 Properties of leading compounds[a]

Compd	HLM/RLM/MLM $T_{1/2}$ (min)[b]	Human PPB (% bound)[c]	Mean P_{app} (10–6 cm s^{-1}) A to B	B to A	Efflux ratio
1a	72/15.6/9.4	90.7	10.59	7.23	0.68
2d	29.7/9.4/6.9	92.5	9.46	5.04	0.53
2h	0.6/17.4/0.6	99.8	0.10	0.15	1.59
3b	10.1/27.5/28.9	>99	1.01	0.93	0.92
3c	7.7/15.4/19.0	>99	0.42	0.37	0.88
3n	7.5/8.9/16.7	99.4	5.14	4.55	0.89
3o	61.4/100.9/104.7	98.6	9.67	3.58	0.37
BTZ043	46.1/22.0/16.7	99.4	9.02	7.17	0.79
PBTZ169	11.1/14.7/14.4	99.6	0.74	0.74	1

[a] Permeability was correlated with the apparent permeability coefficient P_{app} (cm s^{-1}), which was interpreted as follows: low permeability ($P_{app} \leq 1.0 \times 10^{-6}$ cm s^{-1}), moderate permeability ($1.0 \times 10^{-6} < P_{app} < 5.5 \times 10^{-6}$ cm s^{-1}) or high permeability ($P_{app} \geq 5.5 \times 10^{-6}$ cm s^{-1}). [b] HLM = human liver microsomes, RLM = rat liver microsomes, MLM = mouse liver microsomes. [c] PPB = plasma protein binding.

mainly detrimental to activity. Potentially decreased aqueous solubility may be caused by high hydrophobic functionality of benzene ring, so the strategy of bioisostere replacement was used to replacement of benzene ring with hydrophilic group. Pyridine and pyrimidine were designated as high metabolic stability and good hydrophilicity.[24] Pyrimidine-substitution demonstrated stronger activity than pyridine-substitution. *meta* Trifluoromethyl-substitution (**3n**) showed best anti-M.*tb* activity in this group of inhibitors (MIC = 4 nM) but unacceptable aqueous solubility (1.73 μg mL^{-1}). Replacement of the *ortho*-trifluoromethyl group with a *para*-fluorine (**3o**) was investigated to maintain good activity (MIC = 8 nM) with an increased solubility (5.14 μg mL^{-1}). All compounds tested in this series were not toxic to VERO cells up to 10 μ M (CC 50 > 10 μM). Based on the above studies **1a**, **2d**, **2h**, **3b**, **3c**, **3n** and **3o** were selected as representative examples for subsequent validation through resynthesis, retesting, and ADME profiling.

2.2.2 *In vitro* pharmacokinetic studies. Changes in metabolic stability, aqueous solubility and cell permeability/efflux of compound may modulate activity in addition to any changes in target engagement, leading to enormous fluctuations on the bioavailability of drug *in vivo*.[25] *In vitro* pharmacokinetic properties of these selected analogs are summarized in Table 4. As we expected, solubility profiling data of **1a**, **3n**, **3o** indicated that the introduction of ionization center and hydrogen-bond acceptor resulted in a 2–7 fold increase in aqueous solubility relative to **BTZ043**. Compound **2d** showed the prominent aqueous solubility (27.07 μg mL^{-1} in pH = 6.5 and 84.16 μg mL^{-1} in pH = 2.0) of all compounds. However, no solubility increase of **2h**, **3b** and **3c** compared with **BTZ043** were observed, which may be caused by the high hydrophobicity of benzene ring. Further *in vitro* permeability profiling showed that **1a**, **3n** and **3o** had high permeability with $P_{app} > 5.5 \times 10^{-6}$ in MDRI-MDCKII assay, while the permeability of **2h** and **3c** can't be acceptable. With poor aqueous solubility and low permeability, **2h** and **3c** were classified into the fourth group according to Biopharmaceuticals Classification System (BCS). Hence, no further study on these two compounds was carried. Meanwhile, the stabilities of these compounds in microsomes were also be profiled. Compound **2h** showed poor metabolic stability in human liver microsomes (elimination $T_{1/2}$ = 0.6 min), rat liver microsomes (elimination $T_{1/2}$ = 17.4 min) and mice liver microsomes stability (100.9 min) of **3b** (elimination $T_{1/2}$ = 10.1 min) suggests that ester hydrolysis is the main route of metabolism.

Also, the elimination $T_{1/2}$ (29.7 min) of compound **2d** in HLM was 50-fold higher than that of compound **2h** (0.6 min), suggesting the introduction of methyl group in the vicinity of ester

Table 3 Pharmacokinetic parameters for compound **2d**, **3n** and **3o** in SD rat following intravenous and oral administration[a]

	2d		**3n**		**3o**	
Parameters	IV	Oral	IV	Oral	IV	Oral
Dose (mg kg^{-1})	1	10	1	10	1	10
Terminal $T_{1/2}$ (h)	0.78	0.93	10.40	5.01	10.69	9.86
T_{max} (h)	0.08	0.50	0.50	2.00	0.58	2.00
C_{max} (ng mL^{-1})	1057.10	494.83	2310.20	285.40	4179.64	8423.01
$AUC_{0-\infty}$ (ng mL^{-1} h)	421.60	498.60	12 670.46	1657.85	22 666.86	65 818.33
V_z (L kg^{-1})	3.48	—	1.19	—	0.69	—
Cl (L h^{-1} kg)	3.39	—	0.08	—	0.05	—
$MRT_{0-\infty}$ (h)	0.44	1.86	12.71	6.55	12.36	12.58
F (%)	—	11.78	—	1.5	—	29.35

[a] Values are the mean from three animals. Dash indicates that the value was not measured or was not relevant.

Table 4 Pharmacokinetic parameters for compound **3o** and **PBTZ169** in ICR mice mollowing intravenous and oral administration[a]

Parameters	**3o**-IV		**3o**-PO		**PBTZ169**-IV		**PBTZ169**-PO	
Location	Plasma	Tissue	Plasma	Tissue	Plasma	Tissue	Plasma	Tissue
Dose (mg kg^{-1})	10	10	100	100	10	10	100	100
Terminal $T_{1/2}$ (h)	2.62	1.75	2.40	2.84	2.67	3.16	2.09	4.23
T_{max} (h)	1.75	0.08	2.00	2.00	0.08	0.08	2.00	0.50
C_{max} (ng mL^{-1})	5674.10	8872.56	2648.48	4578.33	15 600.40	4208.74	2996.34	811.35
$AUC_{0-\infty}$ (ng mL^{-1} h)	3035.87	5335.01	13 611.26	24 194.36	9074.85	15 146.56	18 882.08	7841.88
V_{ss} (mL kg^{-1})	4524.65	—	—	—	1154.42	—	—	—
Cl (L h^{-1} kg)	3.29	1.87	—	—	1.10	0.66	—	—
$MRT_{0-\infty}$ (h)	1.37	1.08	3.73	4.19	1.05	4.50	3.70	6.50
F (%)	—	—	44.83	45.35	—	—	20.81	5.18

[a] Values are the mean from three animals. Dash indicates that the value was not measured or was not relevant.

bond may improve metabolic stability. Exhilaratingly, compound **3o** showed excellent anti-M.*tb* activity, and good stability across all three species could be noticed with the elimination $T_{1/2}$ in the presence of human liver microsomes (61.4 min), rat microsomes (100.9 min) and mice microsomes (104.7 min). Furthermore, we selected five human CYP450 isoforms CYP1A2, CYP2C9, CYP2C19, CYP2D6 and CYP3A4 for the inhibitory test. Inhibition on CYPs can be detected of compound **1a** (IC_{50} = 8.6 μM for CYP2C19; IC_{50} = 5.33 μM for CYP2A4), 3b (IC_{50} = 6.6 μM for CYP2C19) and **3c** (IC_{50} = 8.6 μM for CYP2C19) (Table S1†). Generally, compounds **1a**, **3c**, **3n** and **3o** exhibited lower protein binding (PPB) compared to **PBTZ169** (Table S2†). The three most promising compounds in *in vitro* pharmacokinetic studies, **2d**, **3n** and **3o**, were selected for the progression into mouse PK studies.

2.2.3 *In vivo* pharmacokinetic studies. With the good anti-M.*tb* activity and favorable druggability *in vitro*, intravenous and oral PK studies – of **2d**, **3n** and **3o** in SD rats were characterized (Table 3). Compound **2d** displayed markedly inferior PK properties (Table 3) with high clearance (Cl = 3.39 L h^{-1} kg) and short terminal $T_{1/2}$ (0.78 h IV, 0.93 h PO). The poor PK is possibly due to its instability in liver microsomes. A long terminal $T_{1/2}$ (5.01 h) when dosed orally indicated an improvement in metabolic stability of **3n**. However, this modification

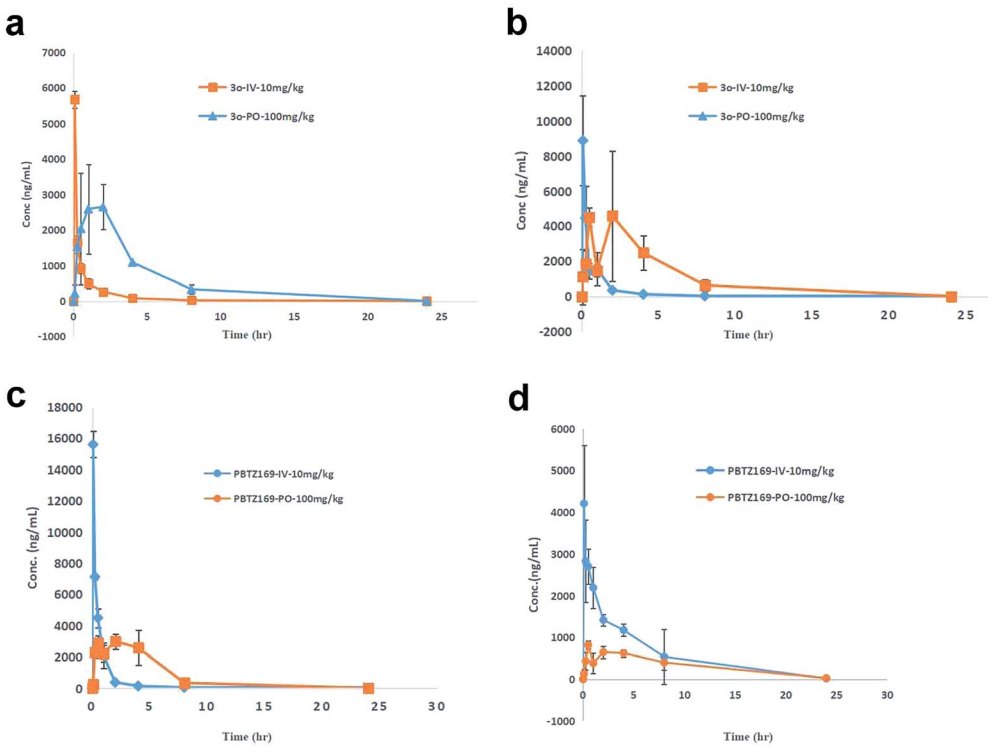

Fig. 2 (a) Mean plasma concentration–time profiles of **3o** after IV and PO dose in ICR mice (n = 3) (mean ± sd). (b) Mean lung concentration–time profiles of **3o** after IV and PO dose in ICR mice (n = 3) (mean ± sd). (c) Mean plasma concentration–time profiles of **PBTZ169** after IV and PO dose in ICR mice (n = 3) (mean ± sd). (d) Mean lung concentration–time profiles of **PBTZ169** after IV and PO dose in ICR mice (n = 3) (mean ± sd).

resulted in poor absorption (*F* 1.54%). Compound **3o** displayed encouraging PK profile in SD rats (Table 3). It exhibited the longest terminal $T_{1/2}$ (9.86 h) among all three compounds, indicating good metabolic stability in SD rats. **3o** displayed good exposure with C_{max} of 2000-fold above the MIC_{90} when dose orally (10 mg kg^{-1}). These results suggested that this modification improved metabolic stability, and resulted in good PK profile.

Then Compound **3o** and **PBTZ169** were subjected to intravenous (10 mg mL^{-1}) and oral (100 mg mL^{-1}) mouse PK (Table 4, Fig. 2a–d). The absorption of **3o** was very good with a bioavailability (*F*) of 44.83% compared with **PBTZ169** (20.81%) (Table 4, S8†). The excellent stability in liver microsomes and lower PPB of **3o** were speculated as important reasons which led the good bioavailability. Furthermore, compound **3o** exhibited more favorable lung enrichment than **PBTZ169**. Generally, compound **3o** displayed near parallel concentration–time profile in plasma (Fig. 2a) and lung tissue (Fig. 2b) whatever intravenous (Tables S3 and S5†) or oral administration. (Tables S4 and S6†), suggesting a rapid equilibrium between these two tissues. **3o** showed almost 4-folds higher absorption in lung than **PBTZ169** (45.35% *vs.* 5.18%) (Tables 4 and S6 and S10†). As the V_{ss} and lung distribution could give an initial indication about a compound's potential for *in vivo* efficacy,[12] the two parameters of compound **3o** were analyzed. Compound **3o** displayed a higher volume of distribution (V_{ss} = 4524.65 mL kg^{-1}) than that of **PBTZ169** (V_{ss} = 1154.42 mL kg^{-1}) resulting in pronounced penetration into tissues (L_{AUC}/P_{AUC} 1.8 and $L_{C_{max}}/P_{C_{max}}$ 1.7) (Tables 4 and S5, S7 and S9†). The duration during which the drug concentration of lungs are above MIC ($T >$ MIC) was selected as an important parameter to estimate *in vivo* efficiency as BTZs are time dependent antimicrobial agents.[4] Compound **3o** displayed $T >$ MIC 100%, which supported to *in vivo* efficiency. The lung concentration–time data following PO administration showed a double peak-shaped curve (Fig. 2b), indicating the possibility of enterohepatic recirculation of **3o** in ICR mice.

3 Conclusion

Optimization of original hit compound **M-1** at position 2 gave series compounds with improved metabolic stability. It provides us a new direction for lead optimization as this very promising scaffold. Screening of these compounds based on PK profile led to the identification of a potent hit compound **3o**, 2-(4-(5-fluoropyrimidin-2-yl)piperidin-1-yl)-6-nitro-8-(trifluoromethyl)-4*H*-benzo[*e*][1,3]thia-zin-4-one. This compound maintained the good anti-*M.tb* activity *in vitro* (MIC = 8 nM) and good metabolic stability in SD rats. The results of PK studies in mice model suggested that **3o** is a promising compound with good exposure and favourable absorptions both in plasma and lung tissue. These foundations may translate to excellent *in vivo* efficacy in the further study of compound **3o** in the TB-mice model. Therefore, compound **3o** was identified as a pre-clinical candidate worthy of further pharmacology and toxicology study *in vivo* in the future.

4 Experimental

4.1 Chemistry

4.1.1 General chemistry. Chemical and reagents were analytical or chemically pure reagents. Organic solvents were dried using the dry solvent system or dried over activated molecular sieves 3 Å. ^{1}H NMR spectra were recorded on Bruker AVANCE^{III} 400 MHz spectrometer. (chemical shifts are given in ppm (δ) relative to TMS (Me_4Si) as the internal standard, coupling constants (*J*) are in hertz (Hz), and signals are designated as follows: s, singlet; d, doublet; t, triplet; m, multiplet; br s, broad singlet, *etc.*). The residual peak of the solvent DMSO-d6 (δ H 2.50 ppm) or $CDCl_3$ (δ H 7.26 ppm) was internal standard for ^{1}H. Mass spectral data were obtained on a Waters Quattro Premier XE spectrometer. TLC was performed on Silica gel 60 F254 with detection by UV light unless staining solution is mentioned.

*4.1.1.1 General procedure for the synthesis of compound **21–24**.* A solution of appropriate amine (**1–4**) (40 mol, eq.), Boc-glycine (7.001 g, 40 mol), HOBt (5400 g, 40 mol) and EDCI (11.502 g, 60 mmol) in dichloromethane (30 mL) was stirred for 12 h. Aqueous hydrochloric acid solution (4 N, 5 mL) was added to the reaction followed by 10 min stir and filtered. The filtrate was washed with a saturated potassium carbonate solution (50 mL × 2). The organic layer was separated, washed by brine, and dried over $MgSO_4$. After filter and removal of the solvent *in vacuo*, the solid was redissolved in trifluoroacetic acid and stirred for 1 h at room temperature. Then, the solvent removed *in vacuo* to yield corresponding trifluoroacetate (93.37%). To a suspension of the trifluoroacetate in dichloromethane (30 mL) and trimethylamine (3 eq.) bath was added 4-nitrobenzenesulfonyl chloride (1.0 eq.) dropwise at 0 °C over a period of 30 min, then stirred for 6 h without cooling. The solvent was evaporated under reduced pressure and added 30 mL water, the mixture was stirred for 30 min and filtered to yield a white solid. Then the solid was dissolved in 10% aqueous sodium hydroxide solution and filtered, the pH was adjusted to 2–3 using a hydrochloric acid solution (6 N). After cooling to room temperature, the solution was filtered and the filter residue (corresponding acetamide) was dried under reduced pressure (85.33%).

Then a solution of the filter residue (1.0 eq.) and potassium carbonate (10.0 eq.) in DMF was stirred at 60 °C for 0.5 h, followed by addition of 1,2-dibromoethane (10 eq.) and the reaction was stirred for another 24 h. The solvent was evaporated under reduced pressure and added 30 mL water, the mixture was stirred for 30 min and filtered to yield a yellow solid (86.68%). (Piperazinone)

Lithium hydroxide (3.0 eq.) was added to a solution of methyl-mercaptopropionate (2.5 eq.) in acetonitrile/DMSO (v/v 49/1), and the mixture was stirred at 50 °C for 30 min. Then, a solution of piperazinone (1.0 eq.) in acetonitrile/DMSO (v/v 49/1) was added dropwise and the reaction was stirred for another 6 h. The solvent removed *in vacuo* to yield crude oil, purification by column chromatography to afford **21–24** (43–74%).

21 (70.51% yield) ^{1}H NMR (400 MHz, $CDCl_3$, Me_4Si) δ 5.03–4.94 (m, 1H), 3.55 (s, 2H), 3.23 (s, 2H), 3.07 (s, 2H), 1.85–1.45 (m, 8H).

24 (71.05% yield) ^{1}H NMR (400 MHz, $CDCl_3$, Me_4Si) δ 4.46 (dd, J = 11.4, 3.6 Hz, 1H), 3.54 (s, 2H), 3.27–3.18 (m, 2H), 3.10–3.00 (m, 2H), 1.79 (s, 2H), 1.76–1.29 (m, 8H).

4.1.1.2 General procedure for the synthesis of compound tert-butyl 4-(8-nitro-4-oxo-6-(trifluoromethyl)-4H-benzo[e][1,3]thiazin-2-yl)piperazine-1-carboxylate. To 3 g of 2-chloro-3-nitro-5-(trifluoromethyl)benzoic acid in dichloromethane 2.64 mL of oxalyl chloride and 0.05 mL DMF were added. The reaction mixture was stirred for 2 h at room temperature. The solvent is removed under reduced pressure, and the residue was dissolved in 25 mL dry dichloromethane. The mixture and 0.2 g of PEG-400 was added to 1.57 g of ammoniumthiocyanate dropwise. It was then stirred at room temperature for 1.5 h. The reaction mixture was filtered. And the filtrate was added to 1.49 g of Boc-piperazine, and it was stirred at room temperature for 40 min. The solvent was evaporated under reduced pressure, and crude product was purified by column chromatography to give yellow solid *tert*-butyl 4-(8-nitro-4-oxo-6-(trifluoromethyl)-4*H*-benzo[*e*][1,3]thiazin-2-yl)piperazine-1-carboxylate (45%).

mp 229.5–232.2 °C. ^{1}H-NMR (400 MHz, DMSO, Me_4Si): δ 9.15 (s, 1H), 9.13 (s, 1H), 3.94 (br s, 4H), 3.53 (br s, 4H), 1.44 (s, 9H); ^{13}C-NMR (DMSO, 400 MHz, Me_4Si): δ 164.72, 161.66, 153.61, 145.33, 144.18, 136.24, 128.83, 125.93, 123.80, 79.47, 45.55, 41.91, 27.98. LC-MS(ESI): m/z 438.1 $(M + H)^+$.

8-Nitro-2-(piperazin-1-yl)-6-(trifluoromethyl)-4*H*-benzo[*e*][1,3]-thiazin-4-one was prepared from *tert*-butyl 4-(8-nitro-4-oxo-6-(trifluoromethyl)-4*H*-benzo[*e*][1,3]thiazin-2-yl)piperazine-1-carboxylate by utilizing TFA in DCM. And then evaporated, extracted by DCM (15 mL × 3). The combined organic layers were washed with a saturated sodium bicarbonate solution and brine, dried over sodium sulfate, and evaporated to afford product 8-nitro-2-(piperazin-1-yl)-6-(trifluoromethyl)-4*H*-benzo[*e*][1,3]thiazin-4-one (85%). LC-MS(ESI): m/z = 347.0 $(M + H)^+$.

*4.1.1.3 General procedure for the synthesis of compound **41–48**.* To a solution of 1-Boc-4-hydroxypiperidine (1.0 eq.) in DCM was dropped slowly appropriate benzoyl chloride (1.1 eq.), followed by addition of trimethylamine (0.1 eq.). The reaction mixture was stirred at room temperature for 1.5–4 h, extracted by a saturated sodium bicarbonate solution. The organic layer was dried over sodium sulfate and evaporated to oil **33–40**. Compounds **41–48** was prepared from **33–40** by utilizing TFA in DCM, and evaporated, dissolved in methyl alcohol. Triethylamine was added to the solution followed by removal of the solvent *in vacuo* to give yellow solid, which used to synthesis of **41–48**.

*4.1.1.4 General procedure for the synthesis of compound **69–78**.* A solution of 1-Boc-4-hydroxypiperidine, appropriate phenol, triphenylphosphine and diethyl azodicarboxylate was stirred in tetrahydrofuran at room temperature for 5 h, evaporated, purified by column chromatography to compounds **59–68**. Compound **69–78** was prepared from **59–68** by utilizing TFA in DCM. Then the solvent was evaporated under reduced pressure, and extracted with DCM. The combined organic layers were washed with a saturated sodium bicarbonate solution and brine, dried over sodium sulfate, filtered and evaporated to afford **69–78**.

*4.1.1.5 General procedure for the synthesis of compound **83, 84, 91–93**.* To a mixture of 1-Boc-4-hydroxypiperidine and sodium hydride was added dry DMSO (10 mL) at 0 °C bath, then stirred for 30 min. A solution of appropriate 2-bromopyridine in dry DMSO was added dropwise at 0 °C, then stirred for 6 h without cooling. The reaction was quenched by adding water (10 mL) and the product extracted with DCM (2 × 10 mL). The combined organic layers were washed with a saturated sodium bicarbonate solution and brine, dried over sodium sulfate, filtered evaporated, and purified by column chromatography to give intermediate **81** and **82**.

83 and **84** were prepared from **81** and **82** by utilizing TFA in DCM. Then the solvent was evaporated under reduced pressure, and extracted with DCM. The combined organic layers were washed with a saturated sodium bicarbonate solution and brine, dried over sodium sulfate, filtered and evaporated to afford **83** and **84**.

Similarly, this condition and appropriate 2-chloropyrimidines, dry *N*,*N*-dimethylformamide were also used for the synthesis of **91–93**.

*4.1.1.6 2-(4-Cyclopentyl-3-oxopiperazin-1-yl)-8-nitro-6(trifluoromethyl)-4H-benzo[e]-[1,3]thiazin-4-one (**1a**).* Method 4.1.2 starting from **1** (54% yield, yellow powder). ^{1}H NMR (400 MHz, DMSO, Me_4Si) δ 9.13 (s, 1H), 8.81 (s, 1H), 4.97 (m, 1H), 4.50 (s, 2H), 4.29 (s, 2H), 3.47 (s, 2H), 1.93 (m, 2H), 1.76 (m, 2H), 1.65 (m, 2H), 1.51 (m, 2H). LC-MS(ESI) LC-MS(ESI): m/z 465.1 $(M + Na)^+$. HPLC purity 99%.

*4.1.1.7 2-(4-Cyclohexyl-3-oxopiperazin-1-yl)-8-nitro-6-(trifluoromethyl)-4H-benzo[e]-[1,3]thiazin-4-one (**1b**).* Method 4.1.2 starting from **2** (51% yield, yellow powder). ^{1}H NMR (400 MHz, $CDCl_3$-$CDCl_3$, Me_4Si) δ 9.13 (d, J = 2.1 Hz, 1H), 8.81 (d, J = 2.0 Hz, 1H), 4.59–4.18 (m, 4H), 3.50 (d, J = 25.1 Hz, 2H), 3.33 (d, J = 7.2 Hz, 1H), 1.75–1.16 (m, 10H). LC-MS(ESI) LC-MS(ESI): m/z 457.1 $(M + H)^+$. HPLC purity 98%.

*4.1.1.8 2-(4-(Cyclohexylmethyl)-3-oxopiperazin-1-yl)-8-nitro-6-(trifluoromethyl)-4H-benzo-[e][1,3]thiazin-4-one (**1c**).* Method 4.1.2 starting from **3** (48% yield, yellow powder). ^{1}H NMR (400 MHz, $CDCl_3$, Me_4Si) δ 9.13 (d, J = 2.1 Hz, 1H), 8.81 (d, J = 2.1 Hz, 1H), 5.30 (s, 1H), 4.60–4.21 (m, 4H), 3.47 (s, 2H), 1.93–1.34 (m, 12H). LC-MS(ESI): m/z 493.1 $(M + Na)^+$. HPLC purity 99%.

*4.1.1.9 2-(4-Butyl-3-oxopiperazin-1-yl)-8-nitro-6-(trifluoromethyl)-4H-benzo[e][1,3]-thiazin-4-one (**1d**).* Method 4.1.2 starting from **4** (62% yield, yellow powder). ^{1}H NMR (400 MHz, DMSO-d6) δ 9.12 (d, J = 6.6 Hz, 1H), 8.81 (d, J = 7.3 Hz, 1H), 4.57 (d, J = 48.4 Hz, 2H), 4.31 (s, 2H), 3.48 (dd, J = 19.1, 11.7 Hz, 4H), 1.66–1.53 (m, 2H), 1.35 (p, J = 7.4, 6.5 Hz, 2H), 1.08–0.88 (m, 3H). LC-MS(ESI): m/z 431.1 $(M + H)^+$. HPLC purity 99%.

*4.1.1.10 Ethyl 1-(8-nitro-4-oxo-6-(trifluoromethyl)-4H-benzo[e][1,3]thiazin-2-yl)piperidine-4-carboxylate (**2a**).* Method 4.1.2 starting from ethyl 4-piperidinecarboxylate (60% yield, yellow powder). ^{1}H NMR (400 MHz, $CDCl_3$, Me_4Si) δ 9.10 (d, J = 2.1 Hz, 1H), 8.77 (d, J = 2.1 Hz, 1H), 4.11 (q, J = 7.1 Hz, 4H), 3.45 (p, J = 5.0 Hz, 1H), 2.75 (m, 4H), 1.24 (t, J = 6.6, 3H). LC-MS(ESI): m/z 454.1 $(M + Na)^+$. HPLC purity 99%.

*4.1.1.11 2Ethyl 2-(4-(8-nitro-4-oxo-6-(trifluoromethyl)-4H-benzo[e][1,3]thiazin-2-yl)-piperazin-1-yl)acetate (**2b**).* Method

4.1.2 starting from 1-(ethoxycarbonylmethyl)piperazine (54% yield, yellow powder). ^{1}H NMR (400 MHz, $CDCl_3$, Me_4Si) δ 9.10 (d, J = 2.1 Hz, 1H), 8.77 (d, J = 2.1 Hz, 1H), 4.21 (q, J = 7.1 Hz, 4H), 3.32 (s, 2H), 2.80 (s, 4H), 1.27 (s, 3H). LC-MS(ESI): m/z 447.1 $(M + H)^+$. HPLC purity 98%.

*4.1.1.12 3Ethyl 2-(1-(8-nitro-4-oxo-6-(trifluoromethyl)-4H-benzo[e][1,3]thiazin-2-yl)-piperidin-4-yl)acetate (**2c**).* Method 4.1.2 starting from ethyl 1-(ethoxycarbonylmethyl)piperidine (47% yield, yellow powder). ^{1}H NMR (400 MHz, $CDCl_3$, Me_4Si) δ 9.20 (d, J = 2.3 Hz, 1H), 8.80 (d, J = 1.9 Hz, 1H), 4.45 (m, 6H), 3.02 (m, 1H), 2.50 (s, 4H), 1.40 (t, J = 6.6 Hz, 3H). LC-MS(ESI): m/z 446.1 $(M + H)^+$. HPLC purity 96%.

*4.1.1.13 Ethyl 2-(4-(8-nitro-4-oxo-6-(trifluoromethyl)-4H-benzo[e][1,3]thiazin-2-yl)-piperazin-1-yl)propanoate (**2d**).* Ethyl 2-bromopropionate (1.5 eq.) was added to a mixture of compound 11(1.0 eq.) and potassium carbonate in dry DMF, the reaction was heated at 60 °C for 3 h followed by pouring in 20 mL water. The reaction mixture was then extracted with DCM (10 mL × 3). The combined organic layers were washed with brine. Dried over sodium sulfate, and the solvent removed *in vacuo* to yield a yellow solid, purification by chromatography to afford **2d** (68%, yellow solid). ^{1}H NMR (400 MHz, $CDCl_3$, Me_4Si) δ 9.03 (d, J = 2.0 Hz, 1H), 8.72 (d, J = 2.0 Hz, 1H), 4.31 (t, J = 7.8 Hz, 2H), 4.22–3.79 (m, 4H), 3.62 (t, J = 7.8 Hz, 2H), 3.18 (s, 4H). ESI HRMS exact mass calcd. For $(C_{18}H_{19}F_3N_4O_5S + Na)^+$ requires m/z 483.09, found m/z 483.0888. HPLC purity 96%.

*4.1.1.14 Ethyl 2-(4-(8-nitro-4-oxo-6-(trifluoromethyl)-4H-benzo[e]-[1,3]thiazin-2-yl)-piperazin-1-yl) butanoate (**2e**).* Method 4.1.24 starting from 2-bromobutanoic acid ethyl ester (58% yield, yellow powder). ^{1}H NMR (400 MHz, $CDCl_3$, Me_4Si) δ 9.04 (s, 1H), 8.72 (s, 1H), 4.90 (dd, J = 7.0, 5.0 Hz, 1H), 4.16 (qd, J = 7.1, 2.5 Hz, 3H), 4.07–3.37 (m, 8H), 1.85 (dt, J = 14.4, 7.3 Hz, 2H), 1.22 (t, J = 7.1 Hz, 3H), 0.95 (t, J = 7.4 Hz, 3H). LC-MS(ESI): m/z 475.1 $(M + H)^+$. HPLC purity 95%.

*4.1.1.15 8-Nitro-2-(4-(2-oxotetrahydrofuran-3-yl)piperazin-1-yl)-6-(tri-fluoromethyl)-4H-benzo[e][1,3]thiazin-4-one (**2f**).* Method 4.1.24 starting from 2-bromo-4-butanolide (63% yield, yellow powder). ^{1}H NMR (400 MHz, $CDCl_3$, Me_4Si) δ 9.20 (d, J = 2.1 Hz, 1H), 8.80 (d, J = 2.1 Hz, 1H), 4.50–3.95 (m, 6H), 3.77–3.60 (m, 1H), 2.66–2.32 (m, 4H), 1.85–1.68 (m, 2H). LC-MS(ESI): m/z 445.1 $(M + H)^+$. HPLC purity 99%.

*4.1.1.16 8-Nitro-2-(4-(2-oxo-5-propyltetrahydrofuran-3-yl) piperazin-1-yl)-6-(trifluoromethyl)-4H-benzo[e][1,3]thiazin-4-one (**2g**).* Method 4.1.24 starting from 3-bromo-5-propyldihydrofuran-2(3*H*)-one (43% yield, yellow powder). ^{1}H NMR (400 MHz, $CDCl_3$, Me_4Si) δ 9.03 (d, J = 2.1 Hz, 1H), 8.70 (d, J = 2.1 Hz, 1H), 4.32–3.84 (m, 5H), 3.69–3.57 (m, 1H), 2.78–2.25 (m, 4H), 1.88–1.66 (m, 2H), 1.57 (ddd, J = 13.9, 9.4, 5.3 Hz, 2H), 1.30–1.00 (m, 2H), 0.90 (dd, J = 8.4, 6.4 Hz, 3H). LC-MS(ESI) m/z 487.1 $(M + H)^+$. HPLC purity 98%.

*4.1.1.17 1-(8-Nitro-4-oxo-6-(trifluoromethyl)-4H-benzo[e][1,3] thiazin-2-yl)piperidin-4-yl 4-fluorobenzoate (**2h**).* Method 4.1.2 starting from 25 (44% yield, yellow powder).^{1}H NMR (400 MHz, $CDCl_3$, Me_4Si) δ 9.04 (dd, J = 2.1, 0.7 Hz, 1H), 8.70 (dd, J = 2.1, 0.7 Hz, 1H), 7.90 (td, J = 7.6, 1.9 Hz, 1H), 7.49 (dddd, J = 8.3, 7.4, 4.9, 1.9 Hz, 1H), 7.17 (dd, J = 7.6, 1.1 Hz, 1H), 7.14–7.03 (m, 1H), 5.39 (p, J = 4.4 Hz, 1H), 4.30–3.79 (m, 4H), 2.00 (d, J = 21.8 Hz, 4H). ESI HRMS exact mass calcd. For $(C_{21}H_{15}F_4N_3NaO_5S + Na)^+$ requires m/z 520.06, found m/z 520.0565. HPLC purity 99%.

*4.1.1.18 1-(8-Nitro-4-oxo-6-(trifluoromethyl)-4H-benzo[e][1,3] thiazin-2-yl)piperidin-4-yl 2-fluorobenzoate (**2i**).* Method 4.1.2 starting from 26 (41% yield, yellow powder). ^{1}H NMR (400 MHz, $CDCl_3$, Me_4Si) δ 9.04 (d, J = 2.2 Hz, 1H), 8.70 (d, J = 2.1 Hz, 1H), 7.89 (tt, J = 7.3, 1.8 Hz, 1H), 7.58–7.45 (m, 1H), 7.14–7.04 (m, 1H), 5.39 (q, J = 4.6 Hz, 1H), 4.41–3.88 (m, 4H), 2.00 (d, J = 24.3 Hz, 4H). LC-MS(ESI): m/z = 498.1$(M + H)^+$. HPLC purity 99%.

*4.1.1.19 1-(8-Nitro-4-oxo-6-(trifluoromethyl)-4H-benzo[e][1,3] thiazin-2-yl)piperidin-4-yl 2-chlorobenzoate (**2j**).* Method 4.1.24 starting from 27 (46% yield, yellow powder). ^{1}H NMR (400 MHz, $CDCl_3$, Me_4Si) δ 9.04 (d, J = 2.1 Hz, 1H), 8.70 (d, J = 2.1 Hz, 1H), 7.86–7.74 (m, 1H), 7.50–7.37 (m, 2H), 7.29 (ddd, J = 8.5, 6.4, 2.2 Hz, 1H), 5.38 (q, J = 4.9 Hz, 1H), 4.02 (d, J = 11.6 Hz, 4H), 2.05 (s, 4H). LC-MS(ESI) m/z 436.0 $(M + Na)^+$. HPLC purity 99%.

*4.1.1.20 1-(8-Nitro-4-oxo-6-(trifluoromethyl)-4H-benzo[e][1,3] thiazin-2-yl)piperidin-4-yl 4-(trifluoromethyl)benzoate (**2k**).* Method 4.1.2 starting from 28 (41% yield, yellow powder). ^{1}H NMR (400 MHz, $CDCl_3$, Me_4Si) δ 9.10 (s, 1H), 8.78 (s, 1H), 7.40 (m, 2H), 7.07 (dd, J = 8.6, 1.1 Hz, 2H), 5.35 (m, 1H), 3.58 (m, 2H), 3.01 (m, 2H), 2.30 (m, 2H), 2.06 (m, 3H). LC-MS(ESI) m/z 548.1 $(M + H)^+$. HPLC purity 98%.

*4.1.1.21 1-(8-Nitro-4-oxo-6-(trifluoromethyl)-4H-benzo[e][1,3] thiazin-2-yl)piperidin-4-yl 4-methoxybenzoat (**2l**).* Method 4.1.2 starting from **29** (43% yield, yellow powder). ^{1}H NMR (400 MHz, $CDCl_3$, Me_4Si) δ 9.10 (dd, J = 2.1, 0.8 Hz, 1H), 8.80–8.73 (m, 1H), 7.02–6.94 (m, 2H), 6.93–6.84 (m, 2H), 5.10–4.27 (m, 2H), 3.80 (s, 3H), 3.56 (t, J = 12.2 Hz, 2H), 2.99 (tt, J = 9.9, 4.2 Hz, 1H), 2.26 (m, 2H), 2.09–1.99 (m, 2H). LC-MS(ESI) m/z 510.1 $(M + H)^+$. HPLC purity 97%.

*4.1.1.22 1-(8-Nitro-4-oxo-6-(trifluoromethyl)-4H-benzo[e][1,3] thiazin-2-yl)piperidin-4-yl 2-methoxybenzoate (**2m**).* Method 4.1.2 starting from **30** (42% yield, yellow powder). ^{1}H NMR (400 MHz, $CDCl_3$, Me_4Si) δ 9.12 (dd, J = 2.1, 0.7 Hz, 1H), 8.80–8.75 (m, 1H), 7.82 (dd, J = 8.0, 1.8 Hz, 1H), 7.54–7.49 (m, 1H), 7.05–6.98 (m, 2H), 5.41 (q, J = 4.4 Hz, 1H), 4.03 (m, 2H), 3.92 (s, 3H), 2.07 (m, 4H), 1.64 (m, 2H). LC-MS(ESI) m/z 510.1 $(M + H)^+$. HPLC purity 99%.

*4.1.1.23 Methyl (1-(8-nitro-4-oxo-6-(trifluoromethyl)-4H-benzo[e][1,3]thiazin-2-yl)-piperidin-4-yl) terephthalate (**2n**).* Method 4.1.2 starting from **31** (46% yield, yellow powder). ^{1}H NMR (400 MHz, $CDCl_3$, Me_4Si) δ 9.05 (dd, J = 2.1, 0.7 Hz, 1H), 8.74–8.69 (m, 1H), 8.09–8.00 (m, 4H), 5.34 (dq, J = 7.0, 3.5 Hz, 1H), 4.22–3.94 (m, 4H), 3.89 (s, 3H), 2.04 (d, J = 55.5 Hz, 4H). LC-MS(ESI) m/z 538.1$(M + H)^+$. HPLC purity 98%.

*4.1.1.24 1-(8-Nitro-4-oxo-6-(trifluoromethyl)-4H-benzo[e][1,3] thiazin-2-yl)piperidin-4-yl 4-(dimethylamino)benzoate (**2o**).* Method 4.1.2 starting from 32 (40% yield, yellow powder). ^{1}H NMR (400 MHz, $CDCl_3$, Me_4Si) δ 9.11 (s, 1H), 8.77 (s, 1H), 7.49–7.41 (m, 1H), 7.34 (m, 1H), 6.99 (dt, J = 8.2, 4.2 Hz, 2H), 5.26 (m, 1H), 4.13–3.92 (m, 4H), 3.34–3.21 (m, 2H), 3.03 (m, 2H), 2.12 (s, 6H). LC-MS(ESI) m/z 523.1$(M + H)^+$. HPLC purity 99%.

*4.1.1.25 2-(4-(2-Fluorophenoxy)piperidin-1-yl)-8-nitro-6-(trifluorom-ethyl)-4H-benzo[e][1,3]-thiazin-4-one (**3a**).* Method 4.1.2 starting from **49** (52% yield, yellow powder). ^{1}H NMR (400 MHz, $CDCl_3$, Me_4Si) δ 9.04 (dd, J = 2.1, 0.7 Hz, 1H), 8.70 (dd, J =

2.1, 0.7 Hz, 1H), 7.90 (td, J = 7.6, 1.9 Hz, 1H), 7.49 (dddd, J = 8.3, 7.4, 4.9, 1.9 Hz, 1H), 7.17 (dd, J = 7.6, 1.1 Hz, 1H), 7.14–7.03 (m, 1H), 5.39 (p, J = 4.4 Hz, 1H), 4.30–3.79 (m, 4H), 2.00 (d, J = 21.8 Hz, 4H). LC-MS(ESI) m/z 493.1(M + Na)$^+$. HPLC purity 99%.

*4.1.1.26 2-(4-(4-Fluorophenoxy)piperidin-1-yl)-8-nitro-6-(trifluoro-methyl)-4H-benzo[e][1,3]-thiazin-4-one (**3b**).* Method 4.1.2 starting from 50 (47% yield, yellow powder). ^{1}H NMR (400 MHz, $CDCl_3$, Me_4Si) δ 9.12 (dd, J = 2.1, 0.8 Hz, 1H), 8.78 (dd, J = 2.1, 0.8 Hz, 1H), 8.12–8.03 (m, 2H), 7.19–7.10 (m, 2H), 5.38 (tt, J = 6.9, 3.6 Hz, 1H), 4.34–3.68 (m, 4H), 2.11 (d, J = 49.2 Hz, 4H). ESI HRMS exact mass calcd. For $(C_{20}H_{19}F_3N_4O_5S + Na)^+$ requires m/z 492.06, found m/z 492.0620. HPLC purity 99%.

*4.1.1.27 2-(4-(3-Fluorophenoxy)piperidin-1-yl)-8-nitro-6-(trifluorome-thyl)-4H-benzo[e][1,3]-thiazin-4-one (**3c**).* Method 4.1.2 starting from 51 (55% yield, yellow powder). ^{1}H NMR (400 MHz, $CDCl_3$, Me_4Si) δ 9.04 (d, J = 2.0 Hz, 1H), 8.70 (d, J = 2.0 Hz, 1H), 7.25–7.19 (m, 1H), 6.70–6.54 (m, 3H), 4.63 (t, J = 4.2 Hz, 1H), 4.17–3.48 (m, 4H), 1.98 (d, J = 10.3 Hz, 4H). LC-MS(ESI): m/z 493.1 (M + Na)$^+$. HPLC purity 99%.

*4.1.1.28 2-(4-(2-Chlorophenoxy)piperidin-1-yl)-8-nitro-6-(trifluo-romethyl)-4H-benzo[e][1,3]thiazin-4-one (**3d**).* Method 4.1.2 starting from 52 (51% yield, yellow powder). ^{1}H NMR (400 MHz, $CDCl_3$, Me_4Si) δ 9.04 (d, J = 2.1 Hz, 1H), 8.70 (d, J = 2.1 Hz, 1H), 7.86–7.74 (m, 1H), 7.50–7.37 (m, 2H), 7.29 (ddd, J = 8.5, 6.4, 2.2 Hz, 1H), 5.38 (q, J = 4.9 Hz, 1H), 4.02 (d, J = 11.6 Hz, 4H), 2.05 (s, 4H). LC-MS(ESI): m/z 486.0 (M + H)$^+$. HPLC purity 96%.

*4.1.1.29 2-(4-(2-Bromophenoxy)piperidin-1-yl)-8-nitro-6-(trifluo-romethyl)-4H-benzo[e][1,3]thiazin-4-one (**3e**).* Method 4.1.2 starting from 53 (46% yield, yellow powder). ^{1}H NMR (400 MHz, $CDCl_3$, Me_4Si) δ 9.03 (d, J = 2.1 Hz, 1H), 8.69 (d, J = 2.1 Hz, 1H), 7.51 (dd, J = 7.9, 1.6 Hz, 1H), 7.26–7.19 (m, 1H), 6.94–6.79 (m, 2H), 4.74 (s, 1H), 2.17–1.84 (m, 4H), 1.55 (s, 4H). LC-MS(ESI) m/z 552.0 (M + Na)$^+$. HPLC purity 97%.

*4.1.1.30 8-Nitro-6-(trifluoromethyl)-2-(4-(2-(trifluoromethyl) pheno-xy)piperidin-1-yl)-4H-benzo[e][1,3]thiazin-4-one (**3f**).* Method 4.1.2 starting from 54 (54% yield, yellow powder). ^{1}H NMR (400 MHz, $CDCl_3$, Me_4Si) δ 9.04 (d, J = 2.1 Hz, 1H), 8.69 (d, J = 2.1 Hz, 1H), 7.55 (dd, J = 7.8, 1.6 Hz, 1H), 7.44 (td, J = 7.9, 1.7 Hz, 1H), 7.03–6.90 (m, 2H), 4.83 (s, 1H), 2.24–1.84 (m, 4H), 1.54 (s, 4H). LC-MS(ESI) m/z 520.1 (M + H)$^+$. HPLC purity 97%.

*4.1.1.31 8-Nitro-2-(4-(o-tolyloxy)piperidin-1-yl)-6-(trifluoro-methyl)-4H-benzo[e][1,3]thiazin-4-one (**3g**).* Method 4.1.2 starting from 55 (57% yield, yellow powder). ^{1}H NMR (400 MHz, $CDCl_3$, Me_4Si) δ 9.04 (d, J = 2.1 Hz, 1H), 8.69 (d, J = 2.1 Hz, 1H), 7.17–7.03 (m, 2H), 6.88–6.72 (m, 2H), 4.67 (s, 1H), 3.88 (s, 4H), 2.19 (s, 3H), 1.99 (s, 4H). LC-MS(ESI) m/z 466.1 (M + H)$^+$. HPLC purity 97%.

*4.1.1.32 8-Nitro-2-(4-(4-(trifluoromethoxy)phenoxy)piperidin-1-yl)-6-(trifluoromethyl)-4H-benzo[e][1,3]thiazin-4-one (**3h**).* Method 4.1.2 starting from 56 (48% yield, yellow powder). ^{1}H NMR (400 MHz, $CDCl_3$, Me_4Si) δ 9.03 (d, J = 2.1 Hz, 1H), 8.70 (d, J = 2.1 Hz, 1H), 7.16–7.06 (m, 2H), 6.92–6.82 (m, 2H), 4.62 (t, J = 4.1 Hz, 1H), 4.37–3.63 (m, 4H), 2.00 (s, 4H). LC-MS(ESI) m/z 536.1 (M + H)$^+$. HPLC purity 96%.

*4.1.1.33 2-(4-(2-Fluoro-4-methylphenoxy)piperidin-1-yl)-8-nitro-6-(tri-fluoromethyl)-4H-benzo[e][1,3]thiazin-4-one (**3i**).* Method 4.1.2 starting from 57 (54% yield, yellow powder). ^{1}H NMR (400 MHz, $CDCl_3$, Me_4Si) δ 9.04 (d, J = 2.1 Hz, 1H), 8.69 (d, J = 2.1 Hz, 1H), 6.92–6.76 (m, 3H), 3.91 (d, J = 25.6 Hz, 4H), 3.42 (s, 1H), 2.23 (s, 3H), 1.94 (s, 4H). LC-MS(ESI) m/z 506.1 (M + Na)$^+$. HPLC purity 98%.

*4.1.1.34 2-(4-(2,6-Difluorophenoxy)piperidin-1-yl)-8-nitro-6-(trifle-oromethyl)-4H-benzo-[e][1,3]thiazin-4-one (**3j**).* Method 4.1.2 starting from 58 (49% yield, yellow powder). ^{1}H NMR (400 MHz, $CDCl_3$, Me_4Si) δ 9.04 (d, J = 2.1 Hz, 1H), 8.69 (d, J = 2.1 Hz, 1H), 7.00–6.80 (m, 3H), 4.50 (s, 1H), 3.98 (s, 4H), 1.97 (d, J = 42.4 Hz, 4H). LC-MS(ESI) m/z 510.1 (M + Na)$^+$. HPLC purity 99%.

*4.1.1.35 8-Nitro-2-(4-(pyridin-2-yloxy)piperidin-1-yl)-6-(trifluoro-methyl)-4H-benzo[e][1,3]thiazin-4-one (**3k**).* Method 4.1.2 starting from 79 (52% yield, yellow powder). ^{1}H NMR (400 MHz, $CDCl_3$, Me_4Si) δ 9.11 (d, J = 2.3 Hz, 1H), 8.78 (d, J = 2.3 Hz, 1H), 8.00 (d, J = 3.4 Hz, 1H), 7.30 (d, J = 8.7 Hz, 1H), 7.15 (d, J = 8.3 Hz, 1H), 7.03(dd, J = 8.6, 3.1 Hz, 1H), 4.72 (p, J = 4.6 Hz, 1H), 4.00 (dt, J = 13.6, 6.3 Hz, 2H), 2.06 (d, J = 16.0 Hz, 4H), 1.35–1.24 (m, 2H). LC-MS(ESI): m/z 475.1 (M + Na)$^+$. HPLC purity 95%.

*4.1.1.36 2-(4-((5-Fluoropyridin-2-yl)oxy)piperidin-1-yl)-8-nitro-6-(tri-fluoromethyl)-4H-benzo[e][1,3]thiazin-4-one (**3l**).* Method 4.1.2 starting from 80 (45% yield, yellow powder).^{1}H NMR (400 MHz, $CDCl_3$, Me_4Si) δ 9.11 (d, J = 2.1 Hz, 1H), 8.78 (d, J = 2.1 Hz, 1H), 8.11 (d, J = 3.1 Hz, 1H), 7.43 (d, J = 8.7 Hz, 1H), 7.15 (dd, J = 8.7, 3.1 Hz, 1H), 4.72 (p, J = 4.3 Hz, 1H), 4.00 (dt, J = 13.6, 6.7 Hz, 2H), 2.06 (d, J = 15.5 Hz, 4H), 1.35–1.24 (m, 2H). LC-MS(ESI): m/z 471.1 (M + Na)$^+$. HPLC purity 98%.

*4.1.1.37 2-(4-((4-Methylpyrimidin-2-yl)oxy)piperidin-1-yl)-8-nitro-6-(trifluoromethyl)-4H-benzo[e][1,3]thiazin-4-one (**3m**).* Method 4.1.2 starting from 85 (58% yield, yellow powder). ^{1}H NMR (400 MHz, $CDCl_3$, Me_4Si) δ 9.11 (d, J = 2.1 Hz, 1H), 8.77 (d, J = 2.1 Hz, 1H), 8.35 (dd, J = 9.2, 5.0 Hz, 1H), 6.85 (d, J = 5.0 Hz, 1H), 4.34 (dd, J = 17.2, 10.2 Hz, 1H), 4.11 (p, J = 6.8 Hz, 4H), 2.48 (d, J = 7.4 Hz, 4H), 1.60 (s, 3H). LC-MS(ESI) m/z 490.1 (M + Na)$^+$. HPLC purity 97%.

*4.1.1.38 8-Nitro-6-(trifluoromethyl)-2-(4-((4-(trifluoromethyl) pyrimidin-2-yl)oxy)piperidin-1-yl)-4H-benzo[e][1,3]thiazin-4-one (**3n**).* Method 4.1.2 starting from 88 (52% yield, yellow powder).^{1}H NMR (400 MHz, $CDCl_3$, Me_4Si) δ 9.11 (d, J = 2.1 Hz, 1H), 8.79 (dd, J = 13.5, 3.5 Hz, 2H), 7.33 (d, J = 4.9 Hz, 1H), 5.50 (p, J = 4.7 Hz, 1H), 4.67–3.90 (m, 4H), 2.17 (s, 4H). ESI HRMS exact mass calcd. For $(C_{19}H_{13}F_6N_5O_3S + Na)^+$ requires m/z 544.05, found m/z 544.0482. HPLC purity 97%.

*4.1.1.39 (4-((4-Chloropyrimidin-2-yl)oxy)piperidin-1-yl)-8-nitro-6-(trifluoromethyl)-4H-benzo[e][1,3]thiazin-4-one (**3o**).* Method 4.1.2 starting from 87 (47% yield, yellow powder).^{1}H NMR (400 MHz, $CDCl_3$, Me_4Si) δ 9.12 (d, J = 2.1 Hz, 1H), 8.78 (d, J = 2.1 Hz, 1H), 8.36 (d, J = 5.7 Hz, 1H), 6.70 (d, J = 5.7 Hz, 1H), 5.57 (tt, J = 6.8, 3.6 Hz, 1H), 4.12 (q, J = 7.2 Hz, 4H), 2.22–2.01 (m, 4H). ESI HRMS exact mass calcd. For $(C_{18}H_{13}F_4O_3S + Na)^+$ requires m/z 494.05, found m/z 494.0526. HPLC purity 99%.

5 Biology

5.1 Mycobacterium tuberculosis H37Ra MIC assay

The MICs against *Mycobacterium tuberculosis* H37Ra were detected by the microplate Alamar blue assay. Compounds were dissolved in dimethyl sulfoxide (DMSO) with concentrations of

1 to 0.002 μmol L^{-1}. *M. tuberculosis* was grown to late log phase in Middlebrook 7H9 medium supplemented with 0.05% Tween 80, 0.2% (vol/vol) glycerol, and 10% (vol/vol) oleic acid-albumin-dextrose-catalase. Cultures were then centrifuged, washed, and resuspended in phosphate-buffered saline. Suspensions were filtrated through an 8 μm-pore-size filter. Then the aliquots were frozen at −80 °C. The number of CFU was determined by plating on 7H11 agar plates. Two-fold dilutions of compounds were prepared in Middlebrook 7H12 medium in a volume of 100 μL in 96-well microplates. *M.tb* (100 μL inoculums of 106 CFU mL^{-1}) was added, the plates were incubated at 37 °C. On the 10th day, add 20 μL 0.01% Alamar Blue and 12.5 μL of 20% Tween 80 to each well. After 24 hours the fluorescence of each well is measured at excitation 530 nm; emission 590 nm.

The MICs were defined as the lowest concentration effecting a reduction in fluorescence of ≥90% relative to the controls. Reported MICs are an average of two or three individual measurements.

5.2 The inhibition to cytochrome P450

CYP inhibition potential of compounds were determined using the following recombinant microsomes: CYP1A2, CYP2C9, CYP2C19, CYP2D6 and CYP3A4. Each incubation (T0, T5, T20, T30, T60, NCF60) which contained recombinant microsomes (80 μL), compounds (10 μL), and extra phosphate buffer (100 mM, pH = 7.4) was added in NCF60. Incubation mixtures were preincubated at 37 °C for 5 minutes, after incubation, 25 mL of NADPH regenerating system solution was added to each well and reactions was started immediately at 37 °C. The reactions were terminated with 300 μL after 60 minutes terminal solution (tolbutamide 100 ng mL^{-1} and labetalol 100 ng mL^{-1}). After centrifugation, the supernatant was analyzed by LC-MS/MS.

5.3 Plasma protein binding rate (PPB) determining

The extent of plasma protein binding for each test compounds was determined by equilibrium dialysis. A 96-well Rapid Equilibrium Dialysis (RED) kit (ThermoFisher Scientific) with cassettes of compounds (pooling of compounds predialysis) was used to perform measurement (each run in triplicate). The plasma was centrifuged (4 minutes, 3500 rpm) and adjusted to pH = 7.4 + 0.1 with 1% phosphoric acid and 1 N sodium hydroxide. Test compound was added to the plasma which was mixed and heated (1 μM, 1% [vol/vol] DMSO, 37 °C). Regenerated cellulose membranes (5000 Daltons, Harvard Apparatus) were soaked in phosphate buffer for 5 minutes and placed within Fast Micro-Equilibrium Dialyzers (Harvard Apparatus). Subsequently, the plasma containing compounds was added to the donor side of the single-use RED plate. Buffer was added to the other side. Equilibrium dialysis was undertaken by incubation (18 hours, 37 °C) and samples were removed from each compartment for LC-MS/MS analysis.

5.4 Pharmacokinetic study

All animal procedures were performed in accordance with the Guidelines for Care and Use of Laboratory Animals of "Experimental Animal management regulations in China" and approved by the Animal Ethics Committee of "Institutional Animal Care and Treatment Committee of Sichuan University, China". SD rats and mice were used in the pharmacokinetic study. Every treatment group contains 3 rats. Animals were dosed with compounds suspension (i.v. and p.o.). Compounds were dissolved in 20% hydroxypropyl-*b*-cyclodextrin (pH = 3.0) for intravenous injection and suspended in 0.1% Tween 80 with 0.5% CMC–Na (pH = 3.0) for oral administration. Blood was collected from the jugular vein of each animal at the following times after administration of drugs: 0.083, 0.25, 0.5, 1, 2, 4, 6, 8 and 24 h after a single IV dosing for SD rats; 0.25, 0.5, 1, 2, 4, 6, 8, 12 and 24 h after a single oral dosing for SD rats; 0.083, 0.25, 0.5, 1, 2, 4, 6, 8 and 24 h after a single IV and oral dosing for ICR mice; all blood samples were centrifuged at 3000 rpm for 10 min to obtain serum which was then stored at −20 °C. 150 μL of the serum was added to 500 μL of acetonitrile and the mixture was centrifuged at 13 000 rpm for 10 min to remove protein. The supernatant was dried and dissolve in 100 μL of acetonitrile, the solution was centrifuged at 13 000 rpm for 10 min.

The supernatant was moved to a sample bottle for HPLC analysis. Pharmacokinetics profile samples were determined directly from the experimental data using WinNonlin V6.2.1.

5.5 Permeability assay

MECK cells were cultured and screened as previous report.[26] Transport assays were conducted using 0.3 mL of apical (AP) donor solution and 1 mL of basolateral (BL) acceptor solution (transport medium). All compounds were tested in three replicate monolayers. Monolayers were incubated with donor and acceptor solutions for 60 min at 37 °C, 95% humidity, with 30 rpm reciprocal shaking. BL compartments were sampled at 15, 30, and 60 min. AP compartments were sampled at 60 min. The quality control compound set (a pool of fenoterol, propranolol and digxin) was assayed as a pool under the same conditions as the test compounds, using a donor solution containing 100 μM of each compound in transport medium (pH 7.4). Most compounds, including the quality control compound set, were quantified by HPLC.

Calculations-P_{app} (apparent permeability) values were calculated according to the following equation:

$$P_{app} = (dQ/dt) \times (1/C_0) \times (1/A)$$

dQ/dt = the permeability rate (calculated by plotting the percent of initial AP drug mass (peak area) found in the BL compartment *versus* time and determining the slope of the line.)

C_0 = the initial concentration in the donor compartment.

A = surface area of the filter.

5.6 Stability in microsomes assay

Previously published incubation procedures using HLM, RLM and MLM were used with modifications.[27] Appropriate substrates and **PBTZ169** (positive controls) were added to incubation tubes. The compounds were individually added in concentration of 10 μM to separate incubation tubes. The

incubation mixtures contained 100 mM phosphate buffer (pH 7.5). The compounds were preincubated with HLMs, RLMs and MLMs (without the index substrates) for 10 minutes at 37 °C, and then followed by 60 min incubation at 37 °C with the substrates (10 μL NADPH). All incubations were performed in duplicate. 300 μL of acetonitrile with (100 ng mL^{-1} tolbutamide and 100 ng mL^{-1} labetalol solution) was used to stop the reactions. After centrifugation, the supernatant was transferred to HPLC vials for HPLC-UV or HPLC-fluorescence analysis.

5.7 Solubility experiment

Previously published method was used with modifications.[28] For solubility experiments with water, an excess amount of solid compounds substance was added to microcentrifuge tubes containing 500 μL of the medium (water with different pH). Reliability of the protocol was confirmed as similar solubilities (RSD < 5%) were obtained in 500 μL medium (microcentrifuge tubes) and 5 mL medium (test tubes) (data not shown). The microcentrifuge tubes were placed at 37 °C in a prewarmed shaking incubator to reach equilibrium. After incubation, samples were centrifuged for 10 min at 14 000 rpm min^{-1} and 37 °C. Subsequently, 100 μL of the supernatant was mixed with 100 μL of methanol (protein precipitation) and centrifuged for 5 min at 14 000 rpm min^{-1} and 37 °C. The supernatant was diluted into the mobile phase used during the subsequent high-performance liquid chromatography (HPLC) analysis.

Conflicts of interest

There are no conflicts to declare.

Acknowledgements

This work was supported by the Natural Science Foundation of China (81703570), China Postdoctoral Science Foundation (2017M612962) and National S&T Major Special Project on Major New Drug Innovations (2018ZX09721001).

References

1 D. B. Giller, B. D. Giller, G. V. Giller, G. V. Shcherbakova, A. B. Bizhanov, I. I. Enilenis and A. A. Glotov, *Eur. J. Cardio Thorac. Surg.*, 2017, DOI: 10.1093/ejcts/ezx447.
2 B. Villemagne, C. Crauste, M. Flipo, A. R. Baulard, B. Deprez and N. Willand, *Eur. J. Med. Chem.*, 2012, **51**, 1–16.
3 T. K. Burki, *Respir. Med.*, 2018, **6**, 13.
4 V. Makarov, G. Manina, K. Mikusova, U. Mollmann, O. Ryabova, B. Saint-Joanis, N. Dhar, M. R. Pasca, S. Buroni, A. P. Lucarelli, A. Milano, E. De Rossi, M. Belanova, A. Bobovska, P. Dianiskova, J. Kordulakova, C. Sala, E. Fullam, P. Schneider, J. D. McKinney, P. Brodin, T. Christophe, S. Waddell, P. Butcher, J. Albrethsen, I. Rosenkrands, R. Brosch, V. Nandi, S. Bharath, S. Gaonkar, R. K. Shandil, V. Balasubramanian, T. Balganesh, S. Tyagi, J. Grosset, G. Riccardi and S. T. Cole, *Science*, 2009, **324**, 801–804.
5 V. Makarov, B. Lechartier, M. Zhang, J. Neres, A. M. van der Sar, S. A. Raadsen, R. C. Hartkoorn, O. B. Ryabova, A. Vocat, L. A. Decosterd, N. Widmer, T. Buclin, W. Bitter, K. Andries, F. Pojer, P. J. Dyson and S. T. Cole, *EMBO Mol. Med.*, 2014, **6**, 372–383.
6 R. Tandon and M. Nath, *Mini Rev. Med. Chem.*, 2017, **17**, 549–570.
7 J. Piton, C. S. Foo and S. T. Cole, *Drug discovery today*, 2017, **22**, 526–533.
8 C. Trefzer, M. Rengifo-Gonzalez, M. J. Hinner, P. Schneider, V. Makarov, S. T. Cole and K. Johnsson, *J. Am. Chem. Soc.*, 2010, **132**, 13663–13665.
9 S. M. Batt, T. Jabeen, V. Bhowruth, L. Quill, P. A. Lund, L. Eggeling, L. J. Alderwick, K. Futterer and G. S. Besra, *Proc. Natl. Acad. Sci. U. S. A.*, 2012, **109**, 11354–11359.
10 M. Brecik, I. Centarova, R. Mukherjee, G. S. Kolly, S. Huszar, A. Bobovska, E. Kilacskova, V. Mokosova, Z. Svetlikova, M. Sarkan, J. Neres, J. Kordulakova, S. T. Cole and K. Mikusova, *ACS Chem. Biol.*, 2015, **10**, 1631–1636.
11 Y. S. Kwon, B. H. Jeong and W. J. Koh, *Curr. Opin. Pulm. Med.*, 2014, **20**, 280–286.
12 S. B. Lakshminarayana, H. I. Boshoff, J. Cherian, S. Ravindran, A. Goh, J. Jiricek, M. Nanjundappa, A. Nayyar, M. Gurumurthy, R. Singh, T. Dick, F. Blasco, C. E. Barry 3rd, P. C. Ho and U. H. Manjunatha, *PLoS One*, 2014, **9**, e105222.
13 K. Lv, X. You, B. Wang, Z. Wei, Y. Chai, B. Wang, A. Wang, G. Huang, M. Liu and Y. Lu, *ACS Med. Chem. Lett.*, 2017, **8**, 636–641.
14 V. Makarov, J. Neres, R. C. Hartkoorn, O. B. Ryabova, E. Kazakova, M. Sarkan, S. Huszar, J. Piton, G. S. Kolly, A. Vocat, T. M. Conroy, K. Mikusova and S. T. Cole, *Antimicrob. Agents Chemother.*, 2015, **59**, 4446–4452.
15 T. Karoli, B. Becker, J. Zuegg, U. Möllmann, S. Ramu, J. X. Huang and M. A. Cooper, *J. Med. Chem.*, 2012, **55**, 7940–7944.
16 T. Maitre, A. Aubry and N. Veziris, *N. Engl. J. Med.*, 2017, **377**, 2403–2404.
17 S. Chong, S. A. Dando and R. A. Morrison, *Pharmaceut. Res.*, 1997, **14**, 1835–1837.
18 A. Aggarwal, M. K. Parai, N. Shetty, D. Wallis, L. Woolhiser, C. Hastings, N. K. Dutta, S. Galaviz, R. C. Dhakal, R. Shrestha, S. Wakabayashi, C. Walpole, D. Matthews, D. Floyd, P. Scullion, J. Riley, O. Epemolu, S. Norval, T. Snavely, G. T. Robertson, E. J. Rubin, T. R. Ioerger, F. A. Sirgel, R. van der Merwe, P. D. van Helden, P. Keller, E. C. Bottger, P. C. Karakousis, A. J. Lenaerts and J. C. Sacchettini, *Cell*, 2017, **170**, 249–259.
19 F. P. Guengerich and W. W. Johnson, *Biochemistry*, 1997, **36**, 14741–14750.
20 M. A. Walker, *Bioorg. Med. Chem. Lett.*, 2017, **27**, 5100–5108.
21 M. Nakajima and Y. zasshi, *J. Pharm. Soc. Jpn.*, 2017, **137**, 697–705.
22 M. J. Fray, D. J. Bull, C. L. Carr, E. C. L. Gautier, C. E. Mowbray and A. Stobie, *J. Med. Chem.*, 2001, **44**, 1951–1962.

23 C. B. Breitenlechner, T. Wegge, L. Berillon, K. Graul, K. Marzenell, W.-G. Friebe, U. Thomas, R. Schumacher, R. Huber, R. A. Engh and B. Masjost, *J. Med. Chem.*, 2004, **47**, 1375–1390.

24 J.-L. Peglion, B. Goument, N. Despaux, V. Charlot, H. Giraud, C. Nisole, A. Newman-Tancredi, A. Dekeyne, M. Bertrand, P. Genissel and M. J. Millan, *J. Med. Chem.*, 2002, **45**, 165–176.

25 U. H. Manjunatha and P. W. Smith, *Bioorg. Med. Chem.*, 2015, **23**, 5087–5097.

26 J. D. Irvine, L. Takahashi, K. Lockhart, J. Cheong, J. W. Tolan, H. E. Selick and J. R. Grove, *J. Pharmaceut. Sci.*, 1999, **88**, 28–33.

27 D. J. Greenblatt, J. S. Harmatz, J. K. Walsh, R. Luthringer, L. Staner, S. Otmani, J. F. Nedelec, C. Francart, S. J. Parent and C. Staner, *Biopharm Drug Dispos.*, 2011, **32**, 489–497.

28 P. Annaert, J. Brouwers, A. Bijnens, F. Lammert, J. Tack and P. Augustijns, *Eur. J. Pharmaceut. Sci.*, 2010, **39**, 15–22.